View metadata, citation and similar papers at core.ac.uk
brought to you by CORE
provided by Carolina Digital Repository

Glycobiology vol. 24 no. 8 pp. 681–692, 2014
doi:10.1093/glycob/cwu032
Advance Access publication on April 25, 2014

Chemoenzymatic synthesis and structural characterization of 2-*O*-sulfated glucuronic acid-containing heparan sulfate hexasaccharides

Po-Hung Hsieh[2], Yongmei Xu[2], David A Keire[3], and Jian Liu[1,2]

[2]Division of Chemical Biology and Medicinal Chemistry, Eshelman School of Pharmacy, University of North Carolina, Rm 303, Beard Hall, Chapel Hill, NC 27599, USA and [3]Food & Drug Administration, CDER (Center for Drug Evaluation and Research), Division of Pharmaceutical Analysis, 645 S Newstead Avenue, St. Louis, MO 63110, USA

Received on January 6, 2014; revised on April 7, 2014; accepted on April 19, 2014

Heparan sulfate and heparin are highly sulfated polysaccharides that consist of a repeating disaccharide unit of glucosamine and glucuronic or iduronic acid. The 2-*O*-sulfated iduronic acid (IdoA2S) residue is commonly found in heparan sulfate and heparin; however, 2-*O*-sulfated glucuronic acid (GlcA2S) is a less abundant monosaccharide (∼<5% of total saccharides). Here, we report the synthesis of three GlcA2S-containing hexasaccharides using a chemoenzymatic approach. For comparison purposes, additional IdoA2S-containing hexasaccharides were synthesized. Nuclear magnetic resonance analyses were performed to obtain full chemical shift assignments for the GlcA2S- and IdoA2S-hexasaccharides. These data show that GlcA2S is a more structurally rigid saccharide residue than IdoA2S. The antithrombin (AT) binding affinities of a GlcA2S- and an IdoA2S-hexasaccharide were determined by affinity co-electrophoresis. In contrast to IdoA2S-hexasaccharides, the GlcA2S-hexasaccharide does not bind to AT, confirming that the presence of IdoA2S is critically important for the anticoagulant activity. The availability of pure synthetic GlcA2S-containing oligosaccharides will allow the investigation of the structure and activity relationships of individual sites in heparin or heparan sulfate.

Keywords: chemoenzymatic synthesis / heparan sulfate / heparin / oligosaccharides / sulfotransferase

Introduction

Proteoglycans mediate many protein functions and physiological processes ranging from cell development, differentiation, inflammation, viral or parasite infection, metastasis to cancer (Bishop et al. 2007). Proteoglycans consist of a core protein and various glycosaminoglycans (GAG) side chains. Although the amino acid sequence of the core protein is encoded by a specific gene, the GAG side chains are generated by a non-template enzymatic process (Feyerabend et al. 2006; Carlsson et al. 2008; Victor et al. 2009). Heparin and heparan sulfate (HS) are members of this polysulfated GAG family.

Heparin, a widely used clinical anticoagulant since the 1930s, was the first biopolymeric drug and is one of the few carbohydrate based drugs (Linhardt 2003; Liu et al. 2009). Because of the heterogeneity of heparin sequences, understanding the contribution of a specific sulfated carbohydrate sequence for a given biological activity remains challenging. Heparin is a mixture of polysaccharides and has high polydispersity and polyheterogeneity (Linhardt 2003) as well as flexible structural characteristics (Liu et al. 2009). In addition, heparin is a highly sulfated polysaccharide with an average molecular weight of ∼17 kDa (Sommers et al. 2011) and with a range of chain lengths from 5000 to 50,000 Da (Ahsan et al. 1995). Heparin has repeating disaccharide units consisting of uronic acid (L-iduronic acid, IdoA or D-glucuronic acid, GlcA) linked 1 → 4 to D-glucosamine (GlcN) (Casu 1985), where the glucosamine residues can be either *N*-acetylated (GlcNAc) or sulfated (GlcNS). The GlcN monosaccharide can also contain *O*-sulfo groups, including 6-*O*- and 3-*O*-sulfation, while the GlcA and IdoA residues can be 2-*O*-sulfated. Heparan sulfate (HS) is structurally analogous to heparin. HS has a similar disaccharide repeating structure to heparin with some noticeable differences. Generally, the HS chains are longer with an average MW of 30 kDa (Griffin et al. 1995), and HS contains a higher GlcA content and less sulfation than heparin (Linhardt 2003). In addition, heparan sulfate has more diverse sulfated saccharide sequences and domain structures compared with heparin.

Reliable structural characterization techniques are critically important to safeguard the quality of heparin drugs. In 2008, batches of contaminated heparin were discovered in United States which drew significant public attention because the contaminated drug killed 94 patients in United States (McMahon et al. 2010). Nuclear magnetic resonance (NMR) techniques were employed and rapidly identified the nature of the contaminant to be over sulfated chondroitin sulfate. This demonstrated the important role of NMR measurements in heparin quality control (Liu et al. 2009). NMR data provide structural information that cannot be obtained by other methods, specifically

[1]To whom correspondence should be addressed: Tel: +1-919-843-6511; e-mail: jian_liu@unc.edu

© The Author 2014. Published by Oxford University Press. All rights reserved. For permissions, please e-mail: journals.permissions@oup.com

epimer recognition, anomeric configuration identification, sulfated position determination and conformation and secondary structure determination. One limitation in utilizing NMR to analyze the structure of heparin or HS is that these species are a mixture of compounds and pure oligosaccharide standards have not been available. Although certain oligosaccharides have been isolated from partially depolymerized heparin or HS, obtaining sufficient amounts of those highly purified oligosaccharides is a difficult and time-consuming process.

Recently, a new method using recombinant HS biosynthetic enzymes to prepare structurally homogeneous HS oligosaccharides was developed (Xu et al. 2011). This method allows the synthesis of a series of structurally homogeneous heparin or HS oligosaccharides at the scale of tens to hundreds of milligram with high yield. Access to highly purified HS oligosaccharides allows for full-scale analyses of these complex molecules by NMR. Notably, these synthetic compounds enable the analysis of structurally "rare" oligosaccharides which are difficult to isolate in sufficient quantity for NMR analysis. For example, the -GlcA2S- residue represents only 1–5% of total uronic acid in heparin isolated from natural sources (Guerrini and Torri 2008).

Here, to address this knowledge gap of the structure characteristics of these potentially important oligosaccharide species, we report the NMR analysis of a series of GlcA2S-containing hexasaccharides with different sulfation patterns. The GlcA2S oligosaccharides were prepared by a chemoenzymatic approach. The GlcA2S NMR data were compared with the data obtained from 2-*O*-sulfated iduronic acid (IdoA2S)-containing oligosaccharides synthesized by the same method. The data confirm previous assignments for the NMR signals of GlcA2S saccharides (Guerrini and Torri 2008).

Results

Chemoenzymatic synthesis of GlcA2S- and IdoA2S-containing hexasaccharides

Total of eight hexasaccharide Constructs **1**–**8** were synthesized in this study using a chemoenzymatic approach (Figure 1). The synthesis was initiated from a commercially available monosaccharide, 1-*O*-(*para*-nitrophenyl) glucuronide (GlcA-pnp), requiring elongation steps, sulfation and epimerization steps (Supplementary data, Figure S1) (Xu et al. 2011). In the synthesis, a hexasaccharide with a structure of GlcNTFA-GlcA-GlcNS-GlcA-GlcNS-GlcA-pnp is a crucial intermediate (Supplementary data, Figure S1). The *N*-trifluoroacetyl group of this hexasaccharide intermediate was hydrolyzed to yield Construct **1** by treatment with lithium hydroxide. Then this hexasaccharide intermediate was treated with a mixture of C5-epi and 2-O-sulfotransferase (OST) to yield a mixture of GlcA2S- and IdoA2S-intermediate (Supplementary data, Figure S1). An anion-exchange HPLC method was used to isolate and purify these two products with a ratio of 1:9 (Figure 2A). After the purification, a GlcA2S-intermediate was obtained with the purity >93% as determined by anion-exchange HPLC (Figure 2B). Similarly, an IdoA2S-intermediate was obtained with the purity >96% (Figure 2C). The GlcA2S-intermediate was further converted to Construct **2** by detriflouroacetylation under an alkaline condition. Additional modifications were made, including *N*-sulfation and 6-*O*-sulfation, yielded to Constructs **3** and **4**, respectively. Similarly, the IdoA2S-intermediate was transformed to Constructs **5**, **6** and **7**. 3-*O*-Sulfation was carried out on Construct **7** to form Construct **8**. The purity analysis of each synthesized oligosaccharide and mass spectrometric analyses are shown in Supplementary data, Figures S2 and S3.

NMR analysis of hexasaccharides

The availability of high-purity structurally defined hexasaccharides provided us sufficient quantities for NMR analyses. The ^{1}H NMR spectra of GlcA-containing hexasaccharide (Construct **1**) and GlcA2S-containing hexasaccharides, including Constructs **2**, **3** and **4**, are shown in Figure 3; the ^{1}H NMR spectra of IdoA2S-containing hexasaccharides, including Constructs **5**–**8**, are shown in Figure 4. The proton signals from the saccharide residues are highly overlapped and this makes the chemical shift assignment difficult. Therefore, 2D-homonuclear and -heteronuclear correlation spectroscopy analyses (^{1}H–^{1}H COSY, TOCSY, ^{1}H–^{13}C HSQC and HMBC) were conducted; these analyses only partially resolved the overlapped signals. Thus, 2D ^{1}H–^{13}C HSQC–TOCSY NMR experiments (Figure 5) were employed to resolve these overlapped signals. The full proton and carbon chemical shift assignments for Constructs **1**–**8** are listed in Tables I and II.

Characterization of GlcA2S-containing oligosaccharides

Here, we use Construct **3** (with the structure of GlcNS-GlcA-GlcNS-GlcA2S-GlcNS-GlcA-pnp) to demonstrate how the signals of GlcA2S were identified in the synthetic oligosaccharides. In the ^{1}H NMR spectrum of Construct **3**, the signals from anomeric protons of the three GlcNS units are located ~5.6 ppm and the signals from GlcA/GlcA2S are located ~4.6 ppm (Figure 3). The ~5.3 ppm shift of I-1 is attributed to the effect of the nearby electron withdrawing group, *para*-nitrophenyl (pnp). The $^{3}J_{HH}$ coupling constants of I-1, III-1 and V-1 were ~8 Hz (consistent with β linkages), and II-1, IV-1 and VI-1 were ~4 Hz (consistent with α linkages). Other saccharide ring proton signals were highly overlapped and resonated between 3.2 and 4.1 ppm. The increased shift dispersion in 2D ^{1}H–^{13}C HSQC–TOCSY NMR, fully resolved these signals so that assignments could be made (Figure 5). In addition, longer ^{1}H–^{1}H COSY and ^{1}H–^{13}C HSQC experiments were run with more points in the indirect dimension for better digital resolution which allowed more accurate identification of the proton and carbon assignments (Table I). The assignments for other GlcA2S-containing hexasaccharides were conducted in a similar manner.

The 2D–^{1}H–^{13}C HMBC experiment confirmed the glycosidic linkages between each saccharide unit through ^{3}J correlations between the anomeric II-1, III-1, IV-1, V-1 or VI-1 protons show connectivity to the I-4, II-4, III-4, IV-4 or V-4 carbons, respectively (Figure 6). These connectivities allowed sequencing of the hexasaccharides. In addition, the anomeric I-1 proton shows a $^{3}J_{CH}$-correlation with the quaternary carbon of the pnp tag. Furthermore, the II-6, IV-6 or VI-6 protons shows through-bond connectivity to II-4, IV-4 or VI-4 carbons, respectively, supporting the assignments of glucosamine residues. The other GlcA2S-containing hexasaccharides were characterized by following the same approach. In addition to ^{1}H–^{1}H COSY and

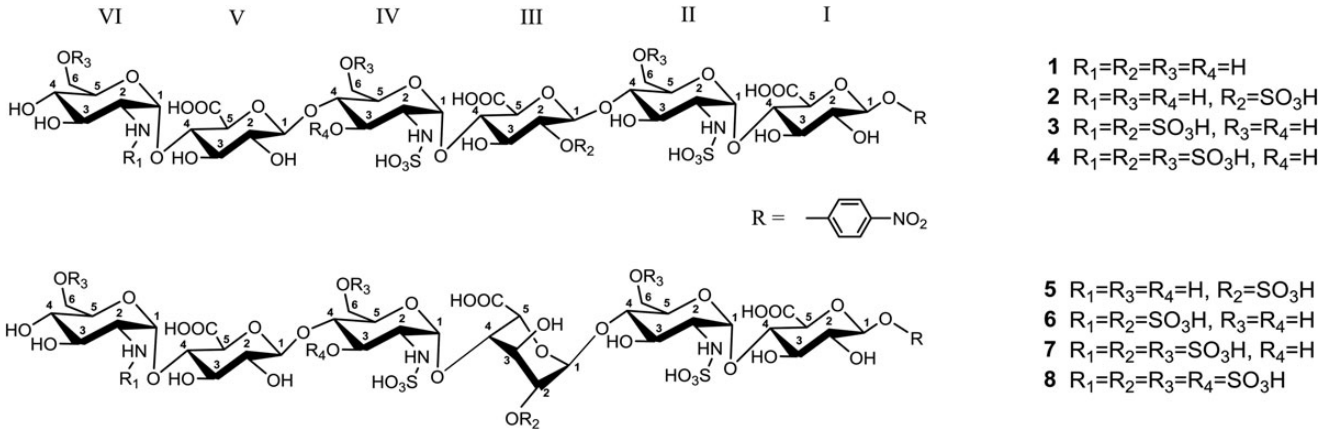

Fig. 1. The synthetic hexasaccharide Constructs **1**–**8**. A total of eight synthetic hexasaccharides were prepared in this study.

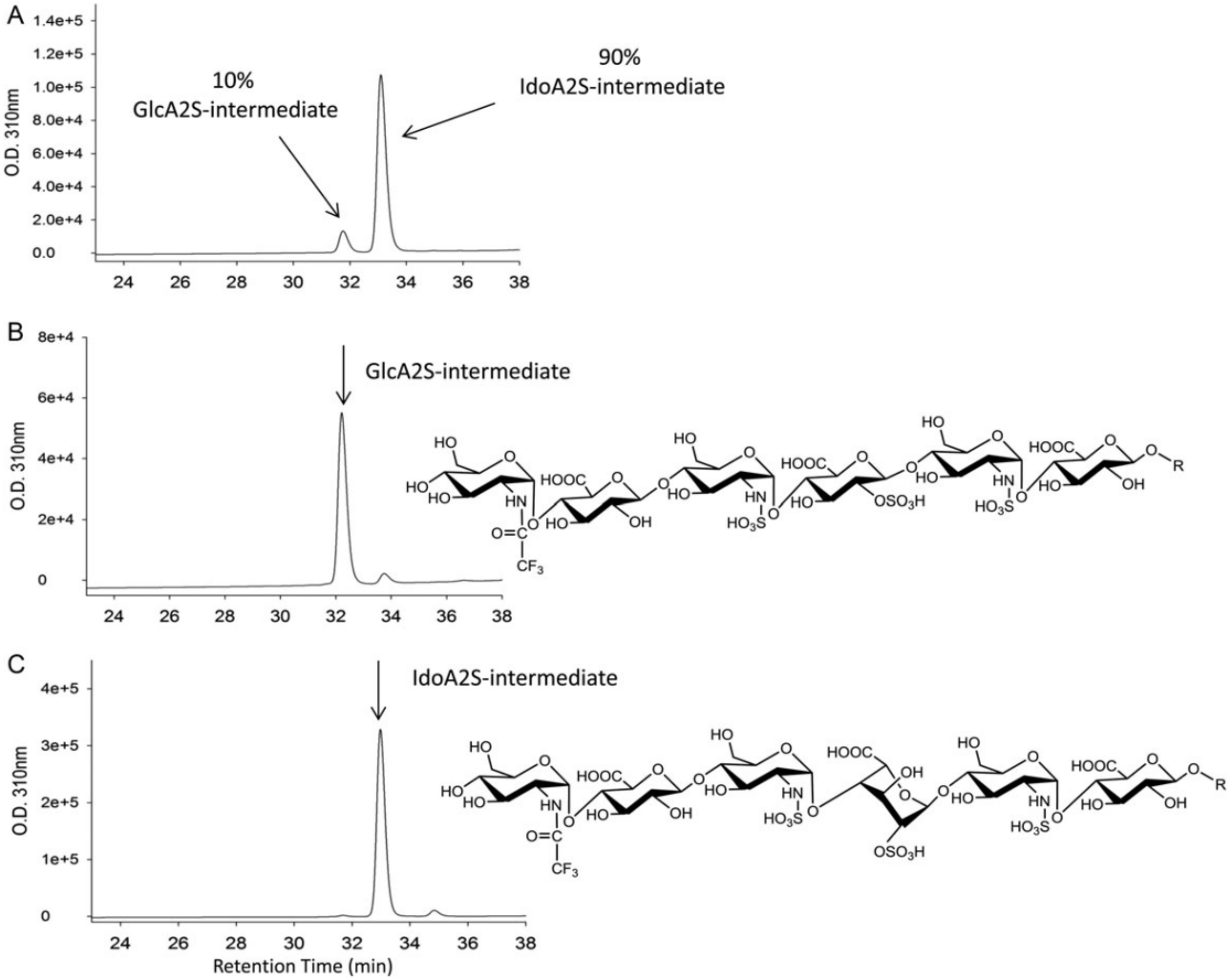

Fig. 2. Two major products of epimerization and 2-*O*-sulfation. (**A**) The anion-exchange HPLC chromatogram after epimerization/2-*O*-sulfation of hexasaccharide intermediate. The product contains 10% GlcA2S-intermediate and 90% IdoA2S-intermediate. (**B** and **C**) The anion-exchange HPLC chromatogram of GlcA2S- and IdoA2S-intermediate after purification. The purity is >93 and 96%, respectively. The chemical structure of GlcA2S- and IdoA2S-intermediate is shown on right of (B) and (C).

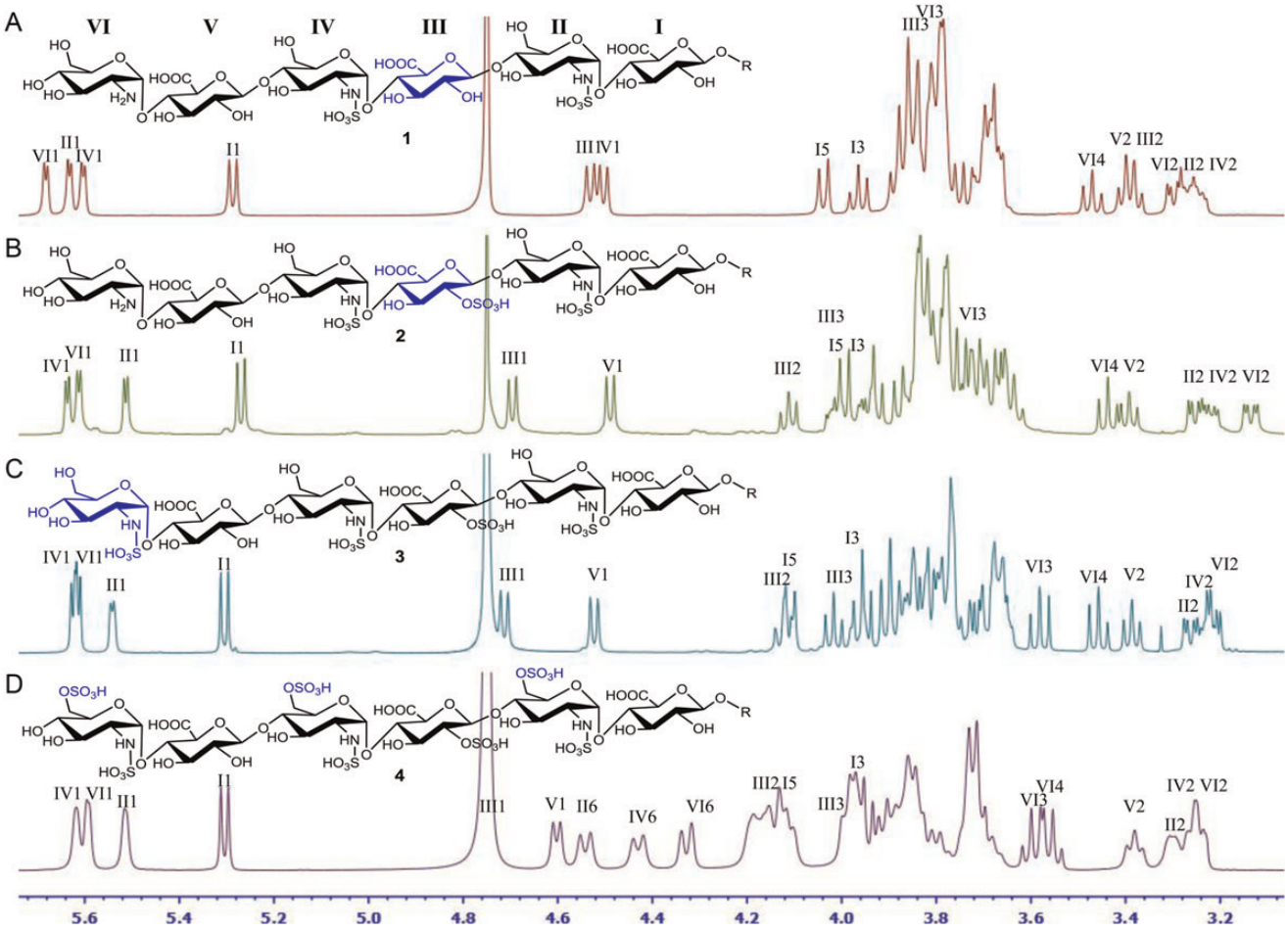

Fig. 3. ^{1}H NMR spectra of Constructs **1**–**4**. (**A**–**D**) The ^{1}H NMR spectrum of Constructs **1**–**4**, respectively. The signals of anomeric protons and some non-overlapping protons are indicated. The chemical structure of construct is shown on top of each panel. The ^{1}H NMR spectra represent the range between 3.1 and 5.7 ppm.

^{1}H–^{13}C HSQC experiments, we focused on using 2D ^{1}H–^{13}C HSQC–TOCSY NMR to identify the residue spin systems and 2D ^{1}H–^{13}C HMBC NMR to confirm the linkages (Figure 3, Table I).

Comparing the NMR spectra of Construct **1** with Construct **2** provides evidence of the influence of 2-*O*-sulfation on the neighboring residues (Figure 3). The signals of III-1, III-2 and III-3 from Construct **2** are shifted +0.17, +0.73 and +0.17 ppm (to 4.70, 4.11 and 4.02 ppm), respectively, due to the attached 2-*O*-sulfo group. Notably, the shift of proton II-1 (−0.12 ppm), II-6b (+0.11 ppm) and VI-2 (−0.15 ppm) are also sensitive to 2-*O*-sulfation even though they are distant from the site of substitution. The chemical shift changes observed for the II residue are attributed to interresidue influences between this additional 2-*O*-sulfo group and cationic groups. The effect on VI-2 may be due to the interactions between the positive charge from the unsubstituted amino group to the nearby 2-*O*-sulfo group. The ~8 Hz axial–axial proton coupling constants of the III residue remain unchanged, indicating that the GlcA2S conformation remains predominately in the $^{4}C_{1}$ form in Construct **2** and is the same as GlcA in Construct **1** (Sattelle et al. 2010).

To reveal the structural flexibility of GlcA2S and IdoA2S residues, we compared the proton spectra of GlcA2S- with IdoA2S-containing hexasaccharides, focusing on the signals of the Residue III. The values of the $^{3}J_{HH}$ coupling constant reflect altered saccharide conformation. The coupling constant (doublet, 8.0 Hz) of III-1 signal of GlcA2S in Construct **2** remains the same as that in Constructs **3** and **4**, suggesting that the conformation of GlcA2S is relatively unaffected by the extra sulfo groups (Figure 3). This result is consistent with that GlcA2S predominately maintain the $^{4}C_{1}$ conformation as GlcA in Construct **1** (Sattelle et al. 2010). We observed that broad signals for IdoA2S (residue III) (Figure 4). The addition of EDTA significantly sharpened the IdoA2S signals (Supplementary data, Figure S5). The spectra show the coupling constants of III-1 signals are altered in different IdoA2S-containing constructs. Similarly, the coupling constants of III-5 signals are also sensitive to different sulfation patterns, suggesting that conformational distribution of IdoA2S is affected by different sulfation pattern. For example, the $^{3}J_{HH}$ coupling constants of III-1 (2.2 Hz) and III-5 (2.2 Hz) signal in Construct **5** are increased to (3.7 Hz) and (3.1 Hz) in Construct **8** due to the presence of additional sulfo groups. These changes are attributed to greater structural flexibility of IdoA2S residue compared to GlcA2S in these constructs. This result is consistent with the

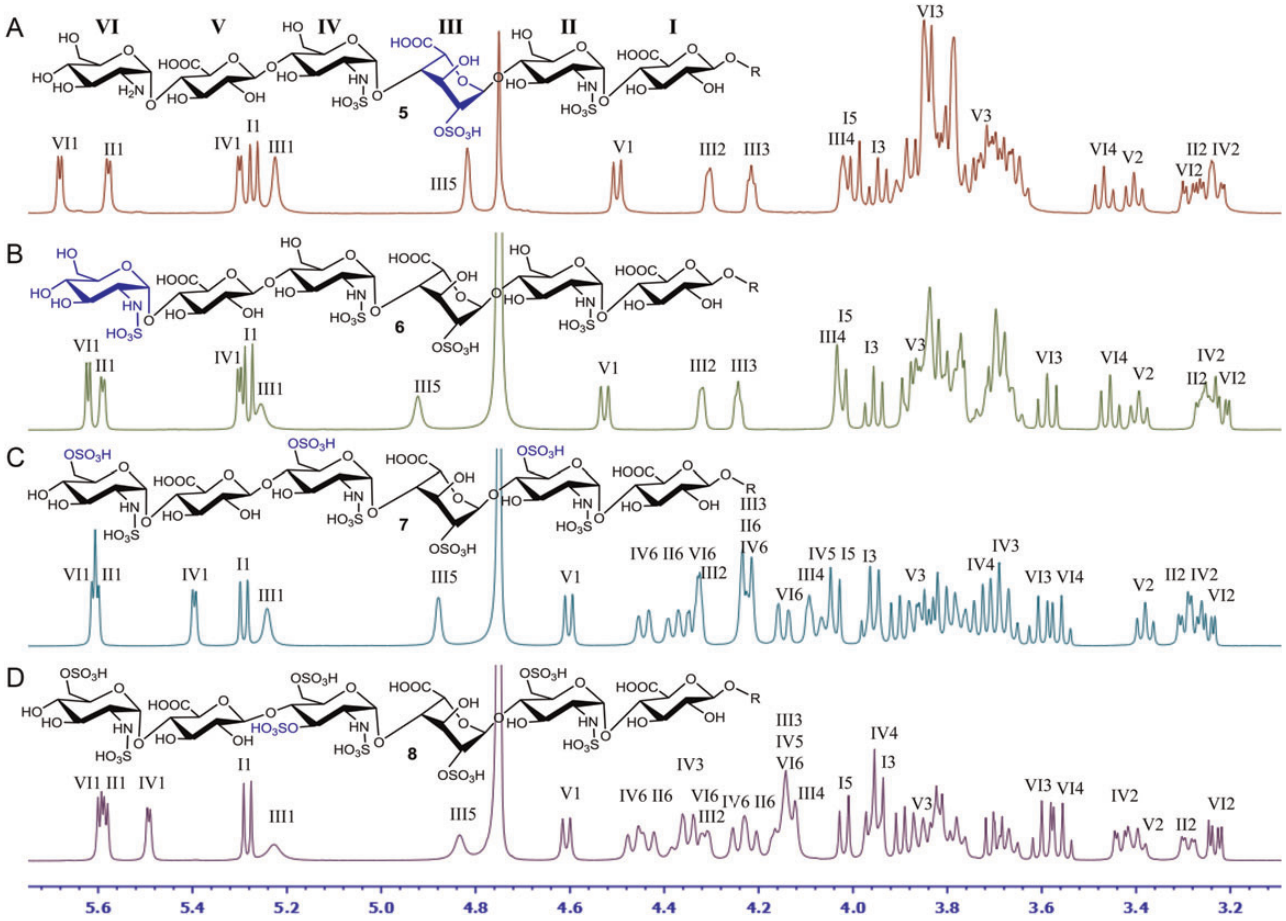

Fig. 4. ^{1}H NMR spectra of Constructs **5**–**8**. (**A**–**D**) The ^{1}H NMR spectrum of Constructs **5**–**8**, respectively. The signals of anomeric protons and some non-overlapping protons are indicated. The chemical structure of construct is shown on top of each panel. The ^{1}H NMR spectra represent the range between 3.1 and 5.7 ppm.

previous reports that IdoA2S equilibrates between $^{2}S_{0}$ (skew boat) and $^{1}C_{4}$ (chair) conformers (Ferro et al. 1990; Sattelle et al. 2010). Although the addition of EDTA did not considerably change the chemical shifts of IdoA2S-containing hexasaccharides, some changes were noted for Construct **5**. In Construct **5**, the VI-2 proton signal shifted by 0.19 ppm with addition of 3 mM EDTA under the same conditions (pD 7.0, 25°C). Similarly, the signals of VI-1 and VI-3 were altered as well (Supplementary data, Table S1).

The presence of GlcA2S or IdoA2S also impacted the chemical environment of neighboring saccharide residues. We compared the signals from each proton of GlcA2S- and IdoA2S-containing hexasaccharides (Table III). As expected, signals from Residue III displayed the largest difference in chemical shifts. Outside Residue III, significant differences in the chemical shifts were observed for the protons of Residue II (II-1, II-3 and II-6), and protons of Residue IV (IV-1 and IV-5) (Table III). For example, comparing the IV-1 proton in Constructs **2** and **5**, the signals are shifted by 0.34 ppm. Similarly, between Constructs **3** and **6** the IV-1 proton was shifted by 0.32 and 0.22 ppm between Constructs **4** and **7**, respectively. These data suggest the presence of GlcA2S or IdoA2S has different effects on the chemical environment of neighboring residues. Beyond Residues II and IV, chemical shift differences between GlcA2S- and IdoA2S-hexasaccharides diminished significantly. Some differences in chemical shifts were observed from Residue VI, an *N*-unsubstituted glucosamine residue in Constructs **2** and **5**, suggesting that the presence of a primary amino group ($-NH_2$) of this end residue is sensitive to GlcA2S vs IdoA2S residues.

Intramolecular effects by N-*sulfation, 6*-O-*sulfation and 3*-O-*sulfation*

Comparing the chemical shifts of the signals from hexasaccharides bearing *N*-unsubstituted vs *N*-sulfated Residue VI suggests the intramolecular interaction between the *N*-sulfo groups and the GlcA residue at its reducing end. The chemical shifts of the V-3 signals in Constructs **2** and **3** are shifted by +0.08 ppm; similarly, the signals of the V-3 protons in Constructs **5** and **6** are shifted +0.10 ppm (Tables I and II). These effects may be attributed to the function of the acidic sulfo group masking the basic amino group on the VI residue and altering the chemical environment around the V residue. These observations are consistent with molecular dynamics simulation results that showed an interaction between the *N*-sulfo group of Residue VI and the V-3 position of Residue V as proposed by Langeslay et al.

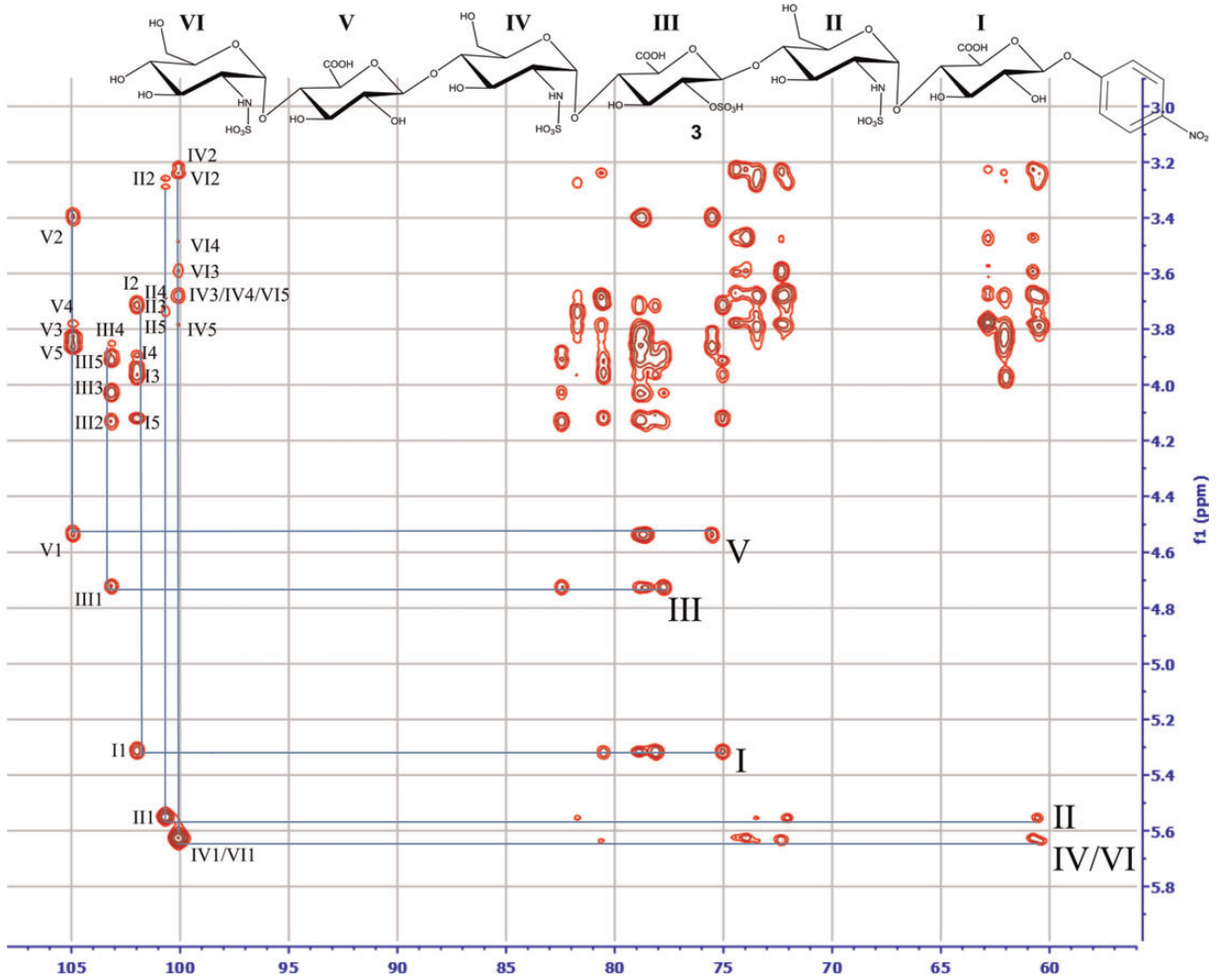

Fig. 5. 2D ^{1}H–^{13}C HSQC–TOCSY NMR spectrum of Construct **3**. 2D ^{1}H–^{13}C HSQC–TOCSY NMR experiment was employed to characterize the structure of Construct **3**. The signals of protons are indicated. The signals are connected with lines identifying correlated protons on each saccharide residue. The chemical structure of Construct **3** is shown on top of the Figure.

(2012) for fondaparinux. Another interesting observation is the impact of *N*-sulfation on the chemical shift of VI-2 signals. In GlcA2S-containing hexasaccharides, *N*-sulfation shifts the VI-2 signal to higher parts per million (+0.06 ppm) due to the effects of de-shielding (less local electron density). In contrast, in IdoA2S-containg hexasaccharides, the *N*-sulfation shifts the VI-2 signal to lower parts per million (−0.07 ppm) due to increased shielding (more electron density). Such different effects suggest more complicated through space interactions between the saccharide residues, which could involve the participation of an IdoA2S or a GlcA2S residue; however, the available techniques do not permit us to dissect these interactions.

As expected, 6-*O*-sulfation clearly shifts the proton resonances of Residues II, IV and VI in both GlcA2S- and IdoA2S-containing hexasaccharides (Tables I and II). The presence of 6-*O*-sulfation also affects the chemical environments of the neighboring residues. For instance, Residue V in Construct **4** is flanked by two GlcNS6S resides (Residues IV and VI), the signal of V-1 is shifted by +0.08 ppm in comparison with this signal in Construct **3**. Similarly, a chemical shift difference for the V-1 proton was also observed (+0.07 ppm) between Constructs **6** and **7** (Tables I and II). These data suggest that the impact of 6-*O*-sulfation on the neighboring residues can be observed in both GlcA2S- and IdoA2S-containing hexasaccharides.

The availability of 3-*O*-sulfated Construct **8** and non-3-*O*-sulfated Construct **7** differentiates the impact of 3-*O*-sulfation on the distribution of IdoA2S residue conformers. The 3-*O*-sulfation on Residue IV alters the conformation of its reducing-end IdoA2S residue (Residue III) as demonstrated by changes in the coupling constant of IdoA2S signals. For example, the $^{3}J_{HH}$ coupling constants of III-1 and III-5 are larger in Construct **8** (3.7 Hz, 3.1 Hz) than in Construct **7** (3.0 Hz, 2.7 Hz) (Supplementary data, Figure S5), suggesting an increased proportion of $^{2}S_{0}$ conformation for Residue III in Construct **8**. Indeed, Guerrini et al. (2013) demonstrated that 3-*O*-sulfated glucosamine residue influences the IdoA2S residue conformational equilibrium between $^{1}C_{4}$ and $^{2}S_{0}$.

Contribution of GlcA2S and IdoA2S to the binding affinity of antithrombin

Heparin binds antithrombin (AT) to exert its anticoagulant activity. Within heparin, a unique pentasaccharide sequence, -GlcNS6S-GlcA-GlcNS3S6S-**IdoA2S**-GlcNS6S-, has been

Table I. $^{1}H–^{13}C$ NMR chemical shift assignments (in ppm) of Constructs **1–4** (25°C, D_2O, pD 7.0)

	1	2	3	4	5	6a	6b
Construct **1** ($GlcNH_2$-GlcA-GlcNS-GlcA-GlcNS-GlcA-pnp)							
I	5.29/102.0	3.69/75.1	3.97/78.6	3.89/79.0	4.04/79.1		
II	5.63/99.9	3.28/60.4	3.69/72.1	3.69/80.6	3.81/73.3	3.80/62.1	3.85/62.1
III	4.53/104.8	3.38/75.4	3.85/78.7	3.79/79.0	3.84/78.7		
IV	5.60/99.9	3.25/60.4	3.68/72.1	3.68/80.5	3.79/73.2	3.80/62.1	3.85/62.1
V	4.50/104.8	3.40/75.9	3.75/78.6	3.82/78.7	3.87/78.6		
VI	5.68/97.9	3.30/56.9	3.84/72.1	3.47/71.8	3.71/75.1	3.79/62.4	3.80/62.4
Construct **2** ($GlcNH_2$-GlcA-GlcNS-GlcA2S-GlcNS-GlcA-pnp)							
I	5.27/102.0	3.70/75.1	3.94/78.2	3.88/81.0	4.00/79.8		
II	5.51/100.7	3.25/60.6	3.73/72.2	3.65/81.9	3.82/73.4	3.82/62.1	3.96/62.1
III	4.70/103.3	4.11/82.5	4.02/77.9	3.84/78.9	3.85/79.0		
IV	5.64/99.9	3.22/60.3	3.67/72.4	3.67/80.6	3.81/73.3	3.84/62.1	3.85/62.1
V	4.49/104.9	3.39/75.9	3.75/78.6	3.77/78.7	3.83/78.6		
VI	5.61/98.9	3.15/57.2	3.76/73.3	3.44/72.0	3.73/75.0	3.78/62.6	3.79/62.6
Construct **3** (GlcNS-GlcA-GlcNS-GlcA2S-GlcNS-GlcA-pnp)							
I	5.31/102.0	3.70/75.0	3.95/78.1	3.89/80.5	4.11/78.9		
II	5.54/100.7	3.26/60.5	3.73/72.0	3.66/81.7	3.78/73.5	3.81/62.0	3.96/62.0
III	4.71/103.2	4.12/82.4	4.01/77.7	3.88/78.8	3.90/78.6		
IV	5.62/100.1	3.23/60.4	3.67/72.3	3.67/80.6	3.77/73.4	3.83/62.1	3.86/62.1
V	4.52/104.9	3.39/75.5	3.83/78.6	3.79/79.0	3.86/78.8		
VI	5.61/100.1	3.21/60.8	3.58/73.9	3.45/72.3	3.66/74.4	3.76/62.8	3.78/62.8
Construct **4** (GlcNS6S-GlcA-GlcNS6S-GlcA2S-GlcNS6S-GlcA-pnp)							
I	5.31/102.0	3.72/75.1	3.96/78.2	3.91/81.4	4.12/79.2		
II	5.51/101.0	3.30/60.5	3.73/72.0	3.73/80.3	3.98/71.7	4.18/68.5	4.54/68.5
III	4.76/102.7	4.14/82.4	3.99/77.8	3.86/79.3	3.87/79.1		
IV	5.62/100.2	3.25/60.2	3.69/72.3	3.73/79.7	3.99/71.5	4.19/68.5	4.43/68.5
V	4.60/104.6	3.38/75.6	3.85/78.7	3.81/79.6	3.87/79.0		
VI	5.59/100.3	3.24/60.7	3.61/73.8	3.56/71.7	3.86/72.5	4.15/69.0	4.33/69.0

Table II. $^{1}H–^{13}C$ NMR chemical shift assignments (in ppm) of Constructs **5–8** (25°C, D_2O, pD 7.0)

	1	2	3	4	5	6a	6b
Construct **5** ($GlcNH_2$-GlcA-GlcNS-IdoA2S-GlcNS-GlcA-pnp)							
I	5.27/102.0	3.69/75.1	3.95/78.5	3.87/79.8	4.00/79.6		
II	5.58/100.3	3.25/61.0	3.65/72.5	3.70/79.7	3.79/73.8	3.83/62.4	3.84/62.4
III	5.23/101.8	4.30/77.6	4.22/70.7	4.03/78.4	4.82/71.1		
IV	5.30/99.8	3.23/60.5	3.71/72.2	3.66/80.5	3.90/73.3	3.84/62.3	3.86/62.3
V	4.50/104.8	3.41/75.9	3.74/78.6	3.83/78.7	3.83/78.8		
VI	5.68/97.9	3.29/56.9	3.83/72.2	3.47/71.9	3.72/75.0	3.78/62.5	3.79/62.5
Construct **6** (GlcNS-GlcA-GlcNS-IdoA2S-GlcNS-GlcA-pnp)							
I	5.28/102.0	3.70/75.1	3.96/78.5	3.88/79.7	4.02/79.4		
II	5.59/100.3	3.26/61.0	3.66/72.4	3.70/79.8	3.80/73.8	3.84/62.3	3.84/62.3
III	5.26/101.8	4.32/77.2	4.24/70.3	4.03/78.4	4.92/70.7		
IV	5.30/100.0	3.25/60.4	3.71/72.1	3.69/80.6	3.85/73.4	3.87/62.1	3.87/62.1
V	4.53/104.9	3.39/75.5	3.84/78.6	3.78/78.9	3.82/79.1		
VI	5.62/100.0	3.22/60.8	3.59/73.9	3.45/72.4	3.68/74.4	3.77/62.9	3.77/62.9
Construct **7** (GlcNS6S-GlcA-GlcNS6S-IdoA2S-GlcNS6S-GlcA-pnp)							
I	5.29/102.0	3.71/75.1	3.95/78.5	3.90/79.7	4.04/79.3		
II	5.60/100.3	3.30/60.7	3.67/72.4	3.77/78.5	3.95/71.9	4.22/69.0	4.38/69.0
III	5.24/101.8	4.32/78.3	4.22/71.5	4.09/78.8	4.88/71.7		
IV	5.40/99.6	3.28/60.2	3.69/72.1	3.74/79.7	4.05/71.6	4.22/68.6	4.44/68.6
V	4.60/104.5	3.38/75.5	3.84/78.6	3.78/79.4	3.82/79.0		
VI	5.61/100.3	3.25/60.6	3.61/73.8	3.56/71.7	3.87/72.5	4.15/69.0	4.33/69.0
Construct **8** (GlcNS6S-GlcA-GlcNS3S6S-IdoA2S-GlcNS6S-GlcA-pnp)							
I	5.28/102.0	3.70/75.1	3.96/78.5	3.90/80.0	4.02/79.4		
II	5.58/100.4	3.29/60.8	3.67/72.4	3.78/79.7	3.96/72.0	4.22/69.0	4.43/69.0
III	5.23/102.2	4.31/79.6	4.17/72.8	4.14/78.5	4.83/72.8		
IV	5.49/98.9	3.43/59.4	4.37/78.8	3.96/75.7	4.14/72.3	4.24/68.7	4.46/68.7
V	4.61/103.9	3.39/75.5	3.81/78.2	3.82/79.6	3.82/78.8		
VI	5.60/100.3	3.23/60.7	3.60/73.9	3.56/71.7	3.86/72.5	4.14/69.0	4.34/69.0

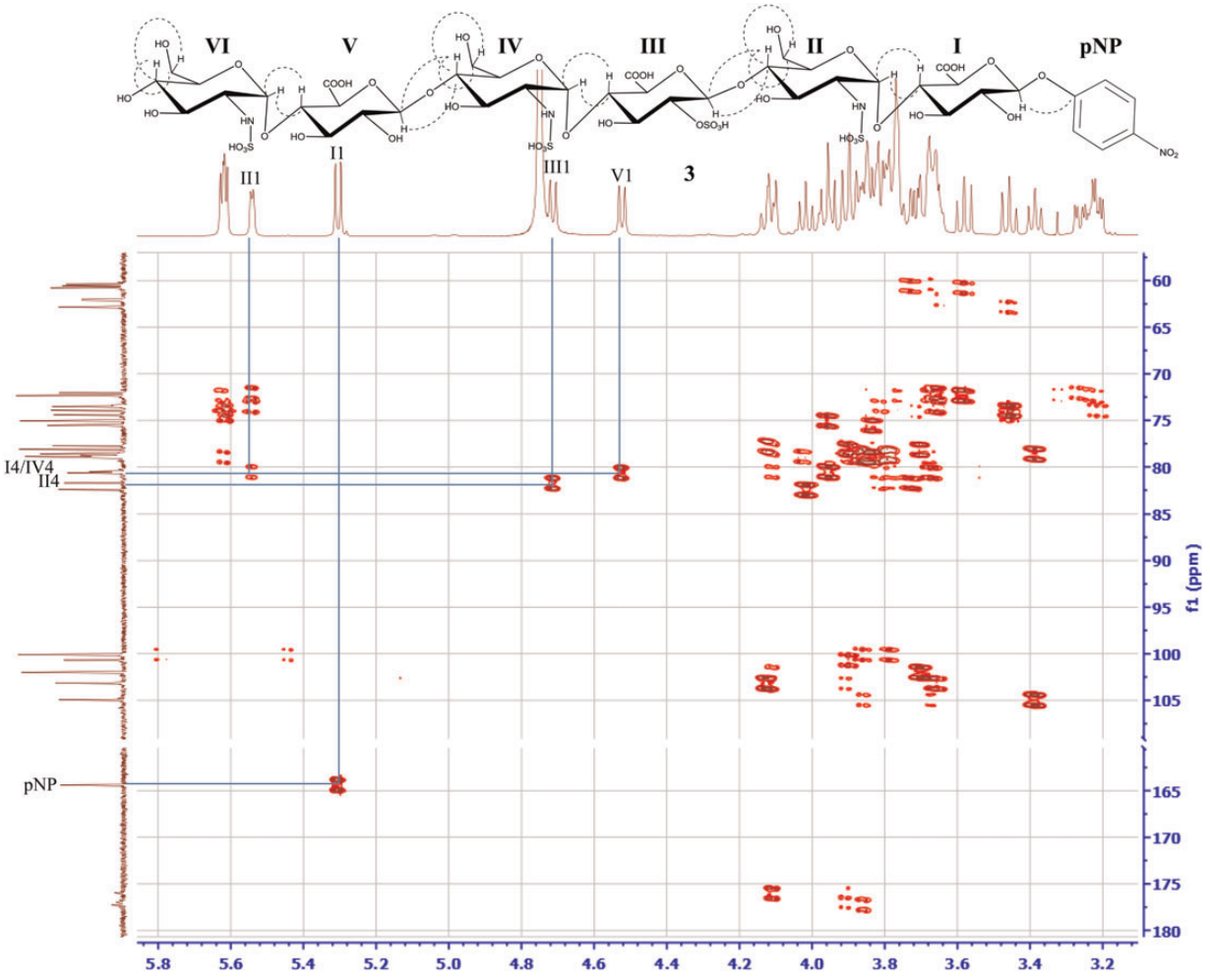

Fig. 6. $^{1}H–^{13}C$ HMBC key correlations of Construct **3**. 2D $^{1}H–^{13}C$ HMBC NMR experiment was employed to confirm the glycosidic linkages between each saccharide unit of Construct **3**. The signals of anomeric protons are indicated. The peaks are connected with lines identifying correlated carbon and proton. The chemical structure of Construct **3** is shown on top of figure. Some other key $^{3}J_{CH}$-correlations are shown as dashed lines on the chemical structure.

shown to display high-binding affinity. Previous work has suggested that IdoA2S in this pentasaccharide domain contributes to the binding of AT (Das et al. 2001). To confirm this conclusion, the binding affinity to AT of the IdoA2S vs GlcA2S constructs was determined. Both 3-*O*-[^{35}S]sulfated GlcA2S- and IdoA2S-containing hexasaccharide were prepared for the analysis. The results showed that IdoA2S-containing hexasaccharide binds to AT with a dissociation constant (K_d) of 12 ± 3 nM, whereas no binding affinity was measurable for GlcA2S-containing hexasaccharide. Our result confirmed the essential role of IdoA2S in AT binding.

Discussion

The GlcA2S residue is present in low abundance in heparin, and thus, very limited information about the role of these rare saccharide residues has been obtained. In this work, we demonstrate the synthesis and structural characterization of highly pure oligosaccharides containing GlcA2S. The synthesis of three GlcA2S-containing hexasaccharides was completed through a chemoenzymatic approach. The substrate specificity of 2-OST modifies only one of the two GlcA in the hexasaccharides, allowing us to position the GlcA2S residue at the desired site (Supplemetary data, Figure S1). Although the synthesis of a number of HS hexasaccharides using a chemical and chemoenzymatic approach has been reported (Petitou and van Boeckel 1992; Liu et al. 2010), the synthesis of the GlcA2S-containing hexasaccharide variants described in this research is novel.

The chemoenzymatic approach allows the construction of diverse hexasaccharide analogs containing an AT-binding domain to confirm the contribution of IdoA2S or GlcA2S residues to AT binding affinity. Our data suggest that GlcA2S-containing hexasaccharides do not bind toAT, despite the fact that they carry 3-*O*- and 6-*O*-sulfo groups, confirming the previously reported essential role of IdoA2S for high-affinity binding to AT (Jin et al. 1997; Hricovini et al. 2001; Guerrini et al. 2010).

The NMR structural analysis data are consistent with the hypothesis that GlcA2S is a relatively structural rigid unit in heparin and HS compared with IdoA2S. The $^{3}J_{HH}$ coupling

Table III. ^{1}H NMR chemical shift difference ($\Delta\delta$) by subtracting GlcA2S- from IdoA2S-containing hexasaccharides[a]

	1	2	3	4	5	6a	6b
Construct **2** vs construct **5**							
I							
II	[+0.07]		[−0.08]				[−0.12]
III	[+0.53]	[+0.19]	[+0.20]	[+0.19]	[+0.97]		
IV	[−0.34]				[+0.09]		
V							
VI	[+0.07]	[+0.14]	[+0.07]				
Construct **3** vs construct **6**							
I					[−0.09]		
II	[+0.05]		[−0.07]				[−0.12]
III	[+0.55]	[+0.20]	[+0.23]	[+0.15]	[+1.02]		
IV	[−0.32]				[+0.08]		
V							
VI							
Construct **4** vs Construct **7**							
I					[−0.08]		
II	[+0.09]		[−0.06]				[−0.16]
III	[+0.48]	[+0.18]	[+0.23]	[+0.23]	[+1.01]		
IV	[−0.22]				[+0.06]		
V							
VI							

[a]Listed values represent chemical shift difference ≥0.05 ppm.

constants of GlcA ring protons in all constructs are ~8.0 Hz as reported previously as $^{4}C_{1}$ form (Sattelle et al. 2010). In our studies, the coupling constant of GlcA2S ring protons in the synthesized hexasaccharide shows equal values, supporting the conformation of GlcA2S remains predominately in the $^{4}C_{1}$ form as well. In contrast, the protons of IdoA2S display smaller coupling constants in the constructs, consistent with the fact that the conformations of the IdoA2S residue are in the equilibrium between $^{2}S_{0}$ and $^{1}C_{4}$ forms.

The $^{2}S_{0}$ conformation of IdoA2S is known to contribute to AT-binding affinity (Hricovini et al. 2001; Guerrini et al. 2008, 2010). Indeed, IdoA2S-containing hexasaccharide displayed high affinity with a K_{d} value of 12 nM, while no detectable AT-binding affinity for GlcA2S-containing hexasaccharide was observed. Importantly, the conformation of the IdoA2S residue can be affected by the protein binding as well as interactions with neighboring sulfated saccharide residues. For example, binding of fibroblast growth factor 1 (FGF1) requires a $^{1}C_{4}$ form of IdoA2S that is flanked by GlcNS6S residues (Faham et al. 1996; DiGabriele et al. 1998; Kreuger et al. 2001); however, in the absence of a nearby GlcNS6S residue, IdoA2S can rearrange its conformation from a $^{2}S_{0}$ to a $^{1}C_{4}$ form which binds FGF2 (Guglier et al. 2008; Zhang et al. 2008). Thus IdoA2S conformation flexibility may play a role in orienting an oligosaccharide for increased binding affinity to a specific protein.

Using highly purified GlcA2S- and IdoA2S-containing hexasaccharides synthesized by the chemoenzymatic approach, we successfully assign all the proton and carbon chemical shifts of GlcA2S- and IdoA2S-containing oligosaccharides through 1D and 2D NMR experiments. We compared the assignments obtained from our study with the previously reported values. The proton assignments of GlcA2S signals in this study are similar to the previous reports, where the GlcA2S residue is flanked by GlcNS6S and GlcNS residue in a tetrasaccharide (Yamada et al. 1995; Limtiaco et al. 2011; Ozug et al. 2012; Guerrini et al. 2013). The anomeric carbon assignment of GlcA2S was also reported (Guerrini and Torri 2008), and our result is consistent with the reported values. In the previous reports, only partial assignments were achieved for the GlcA2S residues. Here, we provide the full assignments for the GlcA2S residue within different sulfated saccharide contexts. The assignments for IdoA2S are consistent with previous reports; however, an IdoA2S residue flanked by two GlcNS3S6S residues shows significant differences in the proton and carbon assignments (Guerrini et al. 2013). The GlcNS3S6S residues may participate in the change of chemical environment and conformation equilibrium of neighboring IdoA2S residue, causing significant chemical shift alterations.

Taking advantage of these chemical shift assignments, the presence of GlcA2S can be easily distinguished from a mixture of GlcA2S- and IdoA2S-containing oligosaccharides within an NMR spectrum. 2D $^{1}H–^{13}C$ HSQC NMR is a powerful tool for fingerprint the GlcA2S residue, and the $^{1}H–^{13}C$ correlation of III-1 and III-2 position signals from this residue is easily observable (Supplementary data, Figure S4). The cross peak of GlcA2S anomeric signal is also consistent to the signal observed in enoxaparin (Guerrini and Torri 2008) or porcine intestinal heparin (Yamada et al. 1995), demonstrating the capability of using the 2D NMR fingerprint method to confirm the authenticity of heparin drugs. Very interestingly, the anomeric signals of GlcA2S were reportedly difficult to identify in unfractionated heparin and low-molecular weight heparins; however, such signals are visible in enoxaparin, a low-molecular weight heparin manufactured by depolymerized unfractionated heparin under basic conditions (Guerrini and Torri 2008; Keire et al. 2013).

Since the 2008 contaminated heparin crisis, NMR analysis of heparin drug has become part of the heparin sodium US Pharmacopeia monograph. Because heparin is a heterogeneous polysaccharide mixture, the assignment of all of the signals is difficult. To this end, acquiring the NMR spectra of highly purified heparin oligosaccharide standards provides a map for assigning highly complex heparin spectra, especially those signals from rare components. Our study should assist NMR analysis of heparin to safeguard this widely used drug.

Materials and methods

Preparation of enzymes and cofactors

Escherichia coli was used for expression of all enzymes: KfiA, pmHS2, NST, C5-epi, 2-OST, 6-OST-1, 6-OST-3 and 3-OST-1 for chemoenzymatic synthesis. Purification was completed by appropriate affinity chromatography as described previously (Xu et al. 2008; Liu et al. 2010). 3′-Phosphoadenosine 5′-phophosulfate (PAPS) is the sulfo donor, was prepared from sodium sulfate and adenosine triphosphate (ATP) utilizing ATP-sulfurylase and adenosine phosphokinase (Zhou et al. 2011). uridine diphosphate (UDP)-GlcNTFA was prepared from glucosamine, followed by reaction with *S*-ethyltrifluorothio acetate and protocol (Liu et al. 2010). GlcNTFA was converted to GlcNTFA-1-phosphate by *N*-acetylhexasamine-1-kinase (Zhao et al. 2010) and subsequently transformed to UDP-GlcNTFA using glucosamine-1-phosphate acetyltransferase/*N*-acetylglucosamine-1-phosphate uridyltransferase (Liu et al. 2010).

Synthesis of hexasaccharide intermediate

The elongation started from a commercial material, GlcA-pnp, followed by elongation of GlcNTFA three times, elongation of GlcA two times, and one detrifluoroacetylation and one *N*-sulfation to make hexasaccharide intermediates (Supplementary data, Figure S1). To introduce a GlcNTFA residue, GlcA-pnp (1.2 mM) was incubated with KfiA (20 μg/mL) in a buffer-containing Tris (25 mM, pH 7.5), $MnCl_2$ (15 mM) and UDP-GlcNTFA (1.5 mM), at room temperature overnight. To introduce a GlcA residue, disaccharide substrate, GlcNTFA-GlcA-pnp (1.2 mM), was incubated with pmHS2 (20 μg/mL) in a buffer-containing Tris (25 mM, pH 7.5), $MnCl_2$ (15 mM) and UDP-GlcA (1.5 mM), at room temperature overnight. C_{18} column (0.75 × 20 cm; Biotage) was used for purification with gradient elution (0–100% acetonitrile in H_2O, 0.1% trifluoroacetyl, 2 mL/min in 60 min). The eluted products were monitored by UV absorbance at 310 nm and characterized by electrospray ionization mass spectrometry (ESI-MS). The additional GlcNTFA and GlcA elongation was repeated under the same condition. Detrifluoroacetylation was completed using 0.1 M LiOH at 0°C for 2 h. The products were analyzed by polyamine-based high-performance liquid chromatography and ESI-MS. Afterwards, *N*-sulfation was performed within pH 7.0 2-(N-morpholino) ethanesulfonic acid (MES) (50 mM), *N*-sulfotransferase (10 μg/mL) and PAPS (0.5 mM, 1.5 equiv. of substrate amount) at 37°C overnight. The sulfated products were purified by Q-Sepharose column (15 × 200 mm, GE Health Sciences) with linear gradient elution (20–100% 1 M NaCl in 20 mM NaOAc, pH 5.0, flow rate 2 mL/min) and followed by dialysis to obtain highly pure hexasaccharide intermediates.

*Synthesis of oligosaccharide Constructs **1**–**8***

Detrifluoroacetylation of hexasaccharide intermediate could get Construct **1**. Constructs **2** and **5** were acquired by epimerization and 2-*O*-sulfation within the solution contained MES (50 mM, pH 7.0), $CaCl_2$ (2 mM), C_5-epi (10 μg/mL), 2-OST (10 μg/mL), PAPS (0.2 mM) and hexasaccharide intermediate (0.13 mM) at 37°C overnight. Following the procedure of *N*-sulfation as described above could synthesize Constructs **3** and **6**. Construct **4** was obtained by 6-*O*-sulfation using PAPS (800 μM), MES (50 mM, pH 7.0), 6-OST-1 (0.6 mg/mL) and 6-OST-3 (0.6 mg/mL) overnight at 37°C. Construct **7** was obtained by 6-*O*-sulfation using PAPS (400 μM), MES (50 mM, pH 7.0), 6-OST-1 (0.1 mg/mL) and 6-OST-3 (0.1 mg/mL) overnight at 37°C. 3-*O*-Sulfation was performed to synthesize Construct **8** under the condition of MES (50 mM, pH 7.0), $MnCl_2$ (10 mM), $MgCl_2$ (5 mM), 3-OST-1 (0.03 μg/mL) and PAPS (600 μM) at 37°C overnight. The purification of Constructs **1**–**8** is essentially the same as the section "Synthesis of hexasaccharide intermediate".

Structural characterization of oligosaccharides

The purity of products was analyzed by polyamine-based anion-exchange (PAMN)-HPLC or diethylethanolamine (DEAE)-HPLC (Figure 2; Supplementary data, Figure S2 and S3). The elution conditions were described in the previous literature (Liu et al. 2010).

Mass spectrometric analyses were performed on all of the intermediates and constructs by ESI-MS (Thermo LCQ-Deca) with direct sample infusion from a syringe pump (Harvard Apparatus). Each sample was diluted in 1:9 MeOH/H_2O and analyzed in negative ionization mode (3.5 kV, 150°C). Xcalibur 1.3 was utilized to acquire and process full scanned MS with 1×10^7 automatic gain control.

The structure of the oligosaccharides constructs and intermediates was analyzed by NMR experiments, including 1D ("s2pul" pulse sequence ^1H or ^{13}C) and 2D (^1H–^1H "gCOSY" pulse sequence COSY, "TOCSY" pulse sequence TOCSY, ^1H–^{13}C "gHSQC" pulse sequence HSQC, "gHMBC" pulse sequence HMBC and "gHSQCTOXY" pulse sequence HSQC–TOCSY) NMR. NMR experiments were performed at 298 K on a Varian Inova 500 MHz spectrometer equipped with 5 mm triple resonance XYZ or broadband PFG probe and processed by VnmrJ 2.2D software. Chemical shifts are referenced to external 2,2-dimethyl-2-silapentane-5-sulfonate sodium salt (Sigma, Co.). Deuterated EDTA (Sigma, Co.) was added to resolve the coupling constants of IdoA2S signals. Samples (5.0–10.0 mg) were each dissolved in 0.5 mL D_2O (99.994%, Sigma, Co.) and lyophilized three times to remove the exchangeable protons. The samples were re-dissolved in 0.5 mL D_2O and transferred to NMR microtubes (OD 5 mm, Norrell). 1D ^1H NMR experiments were performed with 256 scans and an acquisition time of 768 ms. 1D ^{13}C NMR experiments were performed with 40,000 scans, 1.0 s relaxation delay and an acquisition time of 1000 ms. 2D (^1H–^1H COSY, TOCSY, ^1H–^{13}C HSQC and HSQC–TOCSY) spectra were recorded with GARP carbon decoupling, a 1.5 s relaxation delay, a 204 ms acquisition time with 500 increments for 48 scans. Forty-eight steady state scans were used prior to the start of acquisition. A total of 2048 points were collected in f2. Gradients were used for coherence transfer selection with sensitivity enhancement in the HSQC experiment. ^{13}C transmitter offset was set at 77.0 ppm. The echo–anti-echo phase cycling scheme was used. The polarization transfer delay was set with a $^1J_{C-H}$ coupling value of 147 Hz. 2D ^1H–^{13}C HMBC experiments were performed with 72 scans, 1.5 s relaxation delay and a 204 ms acquisition time. The delay for evolution of long-range couplings was set with J_{lr} of 7.6 Hz.

Determination of the binding affinity of oligosaccharides to AT

^{35}S-Labeled 3-*O*-sulfated constructs were prepared via 3-*O*-sulfation as described previously, using [^{35}S]PAPS (0.5 nmol, specific activity 2.2×10^4 cpm/pmol) and oligosaccharide precursor (5 μg) in total 500 μL at 37°C overnight. The products were purified by DEAE-HPLC column. Affinity co-electrophoresis (Lee and Lander 1991) was used for measurement of dissociation constant (K_d) of oligosaccharides. ^{35}S-Labeled 3-*O*-sulfated constructs (1500–2500 cpm) were loaded for lanes with AT concentration at 0, 8, 16, 32, 60, 120, 250, 500 and 1000 nM. The agarose gel was run with 300 mA electrophoresis for 2 h and was dried at room temperature overnight. The dried gel was analyzed by PhosphoImager (Amersham Biosciences, Storm 860). The retardation coefficient was calculated at $R = (M_0 - M)/M_0$, where M_0 is the mobility of the oligosaccharide flow through in the lane without AT, and M is the mobility of the sample in an individual lane. The retardation coefficient was then plotted against the retardation

coefficient divided by its respective AT concentration. The constant $-1/K_d$ is the slope of the trendline.

Supplementary data

Supplementary data for this article are available online at http://glycob.oxfordjournals.org/.

Funding

This work is supported in part by Food and Drug Administration grant U19FD004994 and National Institutes of Health grants HL094463 and GM102137.

Conflict of interest statement

The findings and conclusions in this article have not been formally disseminated by the Food & Drug Administration and should not be construed to represent any Agency determination or policy.

Abbreviations

AT, antithrombin; ATP, adenosine triphosphate; DEAE, diethylethanolamine; ESI-MS, electrospray ionization mass spectrometry; FGF1, fibroblast growth factor 1; GAG, glycosaminoglycans; GlcA, D-glucuronic acid; GlcA2S, 2-*O*-sulfated glucuronic acid; GlcA-pnp, 1-*O*-(*para*-nitrophenyl) glucuronide; GlcN, D-glucosamine; HS, heparan sulfate; IdoA, L-iduronic acid; IdoA2S, 2-*O*-sulfated iduronic acid; MES, 2-(N-morpholino) ethanesulfonic acid; NMR, nuclear magnetic resonance; OST, O-sulfotransferase; PAMN, polyamine-based anion exchange; PAPS, 3′-phosphoadenosine 5′-phophosulfate; pnp, *para*-nitrophenyl; TFA, trifluoroacetyl; UDP, uridine diphosphate.

References

Ahsan A, Jeske W, Hoppensteadt D, Lormeau JC, Wolf H, Fareed J. 1995. Molecular profiling and weight determination of heparins and depolymerized heparins. *J Pharm Sci*. 84(6):724–727.

Bishop JR, Schuksz M, Esko JD. 2007. Heparan sulphate proteoglycans fine-tune mammalian physiology. *Nature*. 446(7139):1030–1037.

Carlsson P, Presto J, Spillmann D, Lindahl U, Kjellen L. 2008. Heparin/heparan sulfate biosynthesis: Processive formation of N-sulfated domains. *J Biol Chem*. 283(29):20008–20014.

Casu B. 1985. Structure and biological activity of heparin. *Adv Carbohydr Chem Biochem*. 43:51–134.

Das SK, Mallet JM, Esnault J, Driguez PA, Duchaussoy P, Sizun P, Herault JP, Herbert JM, Petitou M, Sinay P. 2001. Synthesis of conformationally locked L-iduronic acid derivatives: Direct evidence for a critical role of the skew-boat 2S0 conformer in the activation of antithrombin by heparin. *Chemistry*. 7(22):4821–4834.

DiGabriele AD, Lax I, Chen DI, Svahn CM, Jaye M, Schlessinger J, Hendrickson WA. 1998. Structure of a heparin-linked biologically active dimer of fibroblast growth factor. *Nature*. 393(6687):812–817.

Faham S, Hileman RE, Fromm JR, Linhardt RJ, Rees DC. 1996. Heparin structure and interactions with basic fibroblast growth factor. *Science*. 271 (5252):1116–1120.

Ferro DR, Provasoli A, Ragazzi M, Casu B, Torri G, Bossennec V, Perly B, Sinay P, Petitou M, Choay J. 1990. Conformer populations of L-iduronic acid residues in glycosaminoglycan sequences. *Carbohydr Res*. 195 (2):157–167.

Feyerabend TB, Li JP, Lindahl U, Rodewald HR. 2006. Heparan sulfate C5-epimerase is essential for heparin biosynthesis in mast cells. *Nat Chem Biol*. 2(4):195–196.

Griffin CC, Linhardt RJ, Van Gorp CL, Toida T, Hileman RE, Schubert RL, 2nd, Brown SE. 1995. Isolation and characterization of heparan sulfate from crude porcine intestinal mucosal peptidoglycan heparin. *Carbohydr Res*. 276 (1):183–197.

Guerrini M, Elli S, Gaudesi D, Torri G, Casu B, Mourier P, Herman F, Boudier C, Lorenz M, Viskov C. 2010. Effects on molecular conformation and anticoagulant activities of 1,6-anhydrosugars at the reducing terminal of antithrombin-binding octasaccharides isolated from low-molecular-weight heparin enoxaparin. *J Med Chem*. 53(22):8030–8040.

Guerrini M, Elli S, Mourier P, Rudd TR, Gaudesi D, Casu B, Boudier C, Torri G, Viskov C. 2013. An unusual antithrombin-binding heparin octasaccharide with an additional 3-O-sulfated glucosamine in the active pentasaccharide sequence. *Biochem J*. 449(2):343–351.

Guerrini M, Guglieri S, Casu B, Torri G, Mourier P, Boudier C, Viskov C. 2008. Antithrombin-binding octasaccharides and role of extensions of the active pentasaccharide sequence in the specificity and strength of interaction. Evidence for very high affinity induced by an unusual glucuronic acid residue. *J Biol Chem*. 283(39):26662–26675.

Guerrini M, Torri G. 2008. Quantitative 2D NMR analysis of glycosaminoglycans. In: Holzgrabe U, Diehl B and Wawer I, editors. NMR Spectroscopy in Pharmaceutical Analysis. New York: Elsevier. p. 407–428.

Guglier S, Hricovini M, Raman R, Polito L, Torri G, Casu B, Sasisekharan R, Guerrini M. 2008. Minimum FGF2 binding structural requirements of heparin and heparan sulfate oligosaccharides as determined by NMR spectroscopy. *Biochemistry*. 47(52):13862–13869.

Hricovini M, Guerrini M, Bisio A, Torri G, Petitou M, Casu B. 2001. Conformation of heparin pentasaccharide bound to antithrombin III. *Biochem J*. 359(Pt 2):265–272.

Jin L, Abrahams JP, Skinner R, Petitou M, Pike RN, Carrell RW. 1997. The anticoagulant activation of antithrombin by heparin. *Proc Natl Acad Sci USA*. 94 (26):14683–14688.

Keire DA, Buhse LF, Al-Hakim A. 2013. Characterization of currently marketed heparin products: Composition analysis by 2D-NMR. *Anal Methods*. 5 (12):2984–2994.

Kreuger J, Salmivirta M, Sturiale L, Gimenez-Gallego G, Lindahl U. 2001. Sequence analysis of heparan sulfate epitopes with graded affinities for fibroblast growth factors 1 and 2. *J Biol Chem*. 276(33):30744–30752.

Langeslay DJ, Young RP, Beni S, Beecher CN, Mueller LJ, Larive CK. 2012. Sulfamate proton solvent exchange in heparin oligosaccharides: Evidence for a persistent hydrogen bond in the antithrombin-binding pentasaccharide Arixtra. *Glycobiology*. 22(9):1173–1182.

Lee MK, Lander AD. 1991. Analysis of affinity and structural selectivity in the binding of proteins to glycosaminoglycans: Development of a sensitive electrophoretic approach. *Proc Natl Acad Sci USA*. 88(7):2768–2772.

Limtiaco JF, Beni S, Jones CJ, Langeslay DJ, Larive CK. 2011. The efficient structure elucidation of minor components in heparin digests using microcoil NMR. *Carbohydr Res*. 346(14):2244–2254.

Linhardt RJ. 2003. 2003 Claude S. Hudson Award address in carbohydrate chemistry. Heparin: Structure and activity. *J Med Chem*. 46(13): 2551–2564.

Liu R, Xu Y, Chen M, Weiwer M, Zhou X, Bridges AS, DeAngelis PL, Zhang Q, Linhardt RJ, Liu J. 2010. Chemoenzymatic design of heparan sulfate oligosaccharides. *J Biol Chem*. 285(44):34240–34249.

Liu H, Zhang Z, Linhardt RJ. 2009. Lessons learned from the contamination of heparin. *Nat Prod Rep*. 26(3):313–321.

McMahon AW, Pratt RG, Hammad TA, Kozlowski S, Zhou E, Lu S, Kulick CG, Mallick T, Dal Pan G. 2010. Description of hypersensitivity adverse events following administration of heparin that was potentially contaminated with oversulfated chondroitin sulfate in early 2008. *Pharmacoepidemiol Drug Saf*. 19(9):921–933.

Ozug J, Wudyka S, Gunay NS, Beccati D, Lansing J, Wang J, Capila I, Shriver Z, Kaundinya GV. 2012. Structural elucidation of the tetrasaccharide pool in enoxaparin sodium. *Anal Bioanal Chem*. 403(9):2733–2744.

Petitou M, van Boeckel CA. 1992. Chemical synthesis of heparin fragments and analogues. *Fortschr Chem Org Naturst*. 60:143–210.

Sattelle BM, Hansen SU, Gardiner J, Almond A. 2010. Free energy landscapes of iduronic acid and related monosaccharides. *J Am Chem Soc*. 132 (38):13132–13134.

Sommers CD, Ye H, Kolinski RE, Nasr M, Buhse LF, Al-Hakim A, Keire DA. 2011. Characterization of currently marketed heparin products: Analysis of

molecular weight and heparinase-I digest patterns. *Anal Bioanal Chem*. 401 (8):2445–2454.

Victor XV, Nguyen TK, Ethirajan M, Tran VM, Nguyen KV, Kuberan B. 2009. Investigating the elusive mechanism of glycosaminoglycan biosynthesis. *J Biol Chem*. 284(38):25842–25853.

Xu Y, Masuko S, Takieddin M, Xu H, Liu R, Jing J, Mousa SA, Linhardt RJ, Liu J. 2011. Chemoenzymatic synthesis of homogeneous ultralow molecular weight heparins. *Science*. 334(6055):498–501.

Xu D, Moon AF, Song D, Pedersen LC, Liu J. 2008. Engineering sulfotransferases to modify heparan sulfate. *Nat Chem Biol*. 4(3):200–202.

Yamada S, Murakami T, Tsuda H, Yoshida K, Sugahara K. 1995. Isolation of the porcine heparin tetrasaccharides with glucuronate 2-o-sulfate – heparinase cleaves glucuronate 2-O-sulfate-containing disaccharides in highly sulfated blocks in heparin. *J Biol Chem*. 270(15):8696–8705.

Zhang Z, McCallum SA, Xie J, Nieto L, Corzana F, Jimenez-Barbero J, Chen M, Liu J, Linhardt RJ. 2008. Solution structures of chemoenzymatically synthesized heparin and its precursors. *J Am Chem Soc*. 130(39):12998–13007.

Zhao G, Guan W, Cai L, Wang PG. 2010. Enzymatic route to preparative-scale synthesis of UDP-GlcNAc/GalNAc, their analogues and GDP-fucose. *Nat Protoc*. 5(4):636–646.

Zhou X, Chandarajoti K, Pham TQ, Liu R, Liu J. 2011. Expression of heparan sulfate sulfotransferases in Kluyveromyces lactis and preparation of 3′-phosphoadenosine-5′-phosphosulfate. *Glycobiology*. 21(6): 771–780.